567 (1983); N. Tufillaro, R. Ramshankar, J. Gollub, *Phys. Rev. Lett.* **62**, 422 (1989).
8. Y. Hu, R. E. Ecke, G. Ahlers, *Phys. Rev. E* **48**, 4399 (1993).
9. G. Küppers and D. Lortz, *J. Fluid Mech.* **35**, 609 (1969).
10. R. E. Ecke, Y. Hu, R. Mainieri, G. Ahlers, unpublished data.
11. R. Graham and T. Tél, in *Instabilities and Nonequilibrium Structures III*, E. Tirapegue and W. Zeller, Eds. (Kluwer, Dordrecht, Netherlands, 1991), pp. 125–142.
12. We thank N. Li and M. Cross for useful discussions. Supported by the U.S. Department of Energy and a grant from the Institutional Collaborative Research Program (INCOR), University of California.

13 April 1995; accepted 27 July 1995

Laser Separation of Geometrical Isomers of Weakly Bound Molecular Complexes

Charles Desfrançois, Hassan Abdoul-Carime, C. P. Schulz, Jean Pierre Schermann*

Molecular assemblies held together by weak intermolecular bonds exhibit a rich variety of geometries. Even a simple complex formed by only two molecules can adopt several conformations corresponding to different geometrical isomers. Isomers of small polar dimers can be isolated nondestructively by taking advantage of a selective and reversible ionization process, with the use of a mass spectrometry method that allows the determination and control of the geometrical configuration of neutral or negatively charged molecular complexes in supersonic beams. Here, the method is applied to isolated nucleic acid base pairs that can be selected in stacked or H-bonded configurations.

The understanding of van der Waals or hydrogen interactions under nearly ideal conditions in the gas phase is one of the main purposes of molecular cluster experimental and theoretical studies. Such clusters are usually produced in supersonic beam expansions that yield broad mass distributions. Ionization techniques used in standard mass spectrometry to allow mass selection may strongly modify the initial neutral cluster structures. Nondestructive mass selection of neutral clusters requires sophisticated methods (*1*, *2*); it has been shown that for a given cluster mass, several isomer configurations can still coexist in a beam (*1*, *3*, *4*). The aim of our work here is to show how such isomers can be spatially separated; to achieve this, we had to find parameters that are strongly sensitive to the molecular geometry, allowing ionization processes that do not modify or destroy the selected molecular structure.

In closed-shell polar systems, electrons can be reversibly attached outside the molecular frame, thus providing such a nondestructive ionization process. At large distances r from polar molecules or clusters, excess electrons are attracted by the charge-dipole $-\mu/r^2$ potential (*5*), whereas they suffer repulsion at very short distances. Electrons can thus be trapped in a potential well if the attractive dipole moment μ is larger than 2.5 D (*6*), leading to dipole-bound anions that essentially retain the geometrical configuration of their neutral parents. For example, although single water (μ = 1.854 D) or single ammonia molecules (μ = 1.471 D) are not able to bind excess electrons, a water-ammonia complex can (*7*). The excess electron orbitals are extremely diffuse, and the corresponding electron binding energies are very weak (0.1 to 100 meV). Easily accessible external electric fields (0.1 to 30 kV cm^{-1}) are sufficient to detach the excess electrons (*8*) and therefore allow for a reversible ionizing process. These fragile anions cannot be produced by simple attachment of low-energy free electrons to cold neutral clusters because the presence of a third body is necessary to avoid the reverse process (electron autodetachment). However, dipole-bound anions can be preferentially prepared in collisions between polar systems and highly excited Rydberg atoms in which external electrons are already in very diffuse orbitals; the role of the stabilizing third body is then played by the Rydberg atom ionic core. The signature of the presence of a dipole-bound anion is the appearance of a more or less sharp peak in the anion creation rate as a function of the Rydberg atom orbital size—that is, the principal quantum number n of the Rydberg state (*9*). In contrast, a smooth dependence of the anion rate on n corresponds to the creation of a conventional anion where the excess electron enters a molecular orbital (*10*).

Polar clusters were prepared in a supersonic beam expansion; subsequently, the cluster beam crossed a beam of Rydberg atoms (Fig. 1). Electron exchange took place, and the anions were observed in a time-of-flight setup. An external electric field, created by a set of grids perpendicular to the anion beam (*6*, *8*), can detach the anion excess electron. Above a threshold electric field, which is characteristic of the electron binding energy, anions are transformed back to neutral clusters; this was easily verified by letting them pass through an additional negative repulsive grid. Our mass spectrometry technique can therefore be applied to the production of either charged or neutral geometrically selected complexes.

We can detect only the existence of complexes rather than their geometries, and therefore a comparison between model calculations and experimental measurements of resultant dipole moments is required to deduce structural information. As a first example, let us consider a dimer that results from the mixture of water and acetonitrile molecules. A first experiment (*11*) has shown the existence of a geometrical configuration with a large resultant dipole moment (5.5 D), corresponding to anions that can be produced only by charge exchange with low-lying Rydberg states. This observation was confirmed by a calculation that also

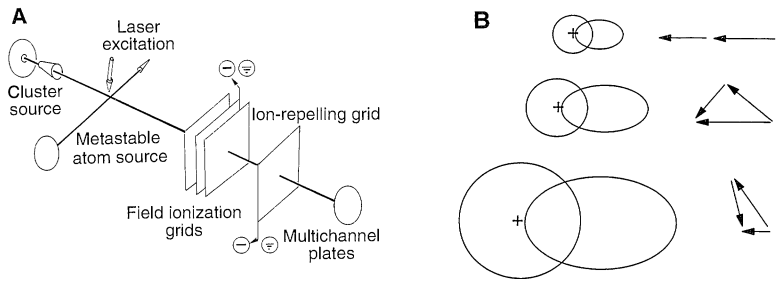

Fig. 1. (**A**) Schematic drawing of the crossed beam experiment used for mass and geometry selection of the different components of a polar cluster beam. Metastable atoms are produced by electron bombardment of xenon (Xe) atoms and are further excited toward Rydberg states by means of a tunable laser. The Rydberg atoms can transfer their external electron to polar clusters, leading to dipole-bound anions. To obtain neutral clusters, we applied an external electric field for detachment of the anion excess electrons. (**B**) Each geometrical configuration of the dipoles corresponds to a resultant dipole moment of the molecular clusters, leading to different dipole-bound anions. In these anions, excess electrons are in diffuse orbitals that are well matched for electron exchange by different Rydberg atom orbitals.

Laboratoire de Physique des Lasers, Université Paris-Nord Villetaneuse 93430, France.

*To whom correspondence should be addressed.

predicted that the mixed $CH_3CN \cdots H_2O$ complex can adopt another configuration with nearly the same binding energy (*11*) but with a much smaller dipole moment (2.6 D). The corresponding electron binding energy is very weak and imposes the use of very weak electric fields in the time-of-flight setup. This second isomer configuration had thus remained unobserved before our experiments here. By tuning the laser for production of Rydberg atoms with a principal quantum number $n = 9$ or $n = 25$, we can selectively produce a beam of dimers with only one of these two well-defined structures (9 and 25 are only approximate numbers; see the spread of peaks in Fig. 2). By means of field detachment, we easily obtained a beam of neutral dimers with the same selected geometries. The potentially reactive nitrogen atom of acetonitrile is "protected" by the water molecule in one case and not in the other, thus offering the possibility of selective chemistry.

We applied this method to nucleic acid bases and base pairs. Most of our understanding of these systems (geometrical configurations, dipole moments, electron affinities) comes from quantum chemistry calculations of isolated (gas-phase) molecules. Hence, we wished to obtain experimental information that would allow direct comparison with theoretical predictions. Canonical (nonmethylated) nucleic acid bases are difficult to vaporize without decomposition. Experimental data are thus scarce and restricted to the observation of thymine anions (T^-) by field ionization (*12*), the determination of the dipole moment of uracil (U) (*13*), and ultraviolet spectroscopy of U and thymine (T) (*14*) in a pulsed supersonic beam, together with the determination of binding energies of methylated base pairs (*15*) and infrared studies of bases isolated in an argon matrix (*16, 17*).

We generated a continuous supersonic beam of canonical U, T, and A (adenine) and some of their pairs. In the analysis of our negative ion mass spectra, a careful mass calibration was performed to ensure the absence of any protonation or deprotonation (Fig. 3). In the case of monomers, we observed that uracil and thymine gave rise to both dipole-bound and conventional anions, whereas adenine formed only dipole-bound anions, which is in good agreement with recent calculations (*18, 19*). We were able to make a direct diagnosis of the onset of chemical decomposition when spurious anion signals appeared at very low electron energies ($n > 25$). The rapid decomposition of cytosine (C) does not allow for the study of the C^- anion or for the observation of the C-G pair.

The question we wish to address here is whether the canonical base pairs isolated in vacuum correspond to the same hydrogen-bonded (H-bonded) pairs (Crick-Watson–Hoogsteen) as in the double-helix structure of DNA or to different H-bonded or stacked pairs. We observed two features of the T-T, U-U, A-A, and A-T anion pair signals. First, the dimer signals have the same linear pressure dependence as the monomer signals. This shows that the parent neutral pairs are not formed by clustering in the gas phase; rather, they result directly from the sublimation of the nucleic acid base powders. Second, we observed the existence of two types of anions for the T-T pair (Fig. 4): dipole-bound anions at low values of n and conventional anions at large values of n. In contrast, only conventional $(U\text{-}U)^-$ and other pair (A-T and A-A) anions were detected.

Nucleic acid base pairs can adopt quasi-planar, H-bonded, or stacked configurations. The only experimentally determined energy differences, $\Delta E = E_{HB} - E_S$, are for methylated bases (where E_{HB} and E_S are the respective binding energies of H-bonded and stacked complexes in the gas phase) (*15*); however, the influence of methylation upon ΔE is far from negligible (*15*). Quantum chemical calculations (*20*) have been performed for stacked pairs and H-bonded pairs, corresponding to those formed in the canonical base solids (*21*). These calculations, which are directly relevant to our experiments here, predict that ΔE is smaller for the T-T pair (2.3 kcal mol^{-1}) than for the U-U pair (3.6 kcal mol^{-1}). This implies that among all isomer configurations that are populated at the high temperature (≈500 K) of the oven, stacked and H-bonded pairs probably coexist for the T-T pair, whereas only H-bonded configurations are created for all other pairs studied here. The different H-bonded T-T pairs correspond to almost antiparallel dipole configurations (*20, 22, 23*) with nearly null resultant dipole moments and thus cannot form the observed dipole-bound anions. This leads us to attribute the observation of $(T\text{-}T)^-$ dipole-bound anions to the presence of thymine stacked pairs in the supersonic beam. The observed different behavior of thymine (base of DNA) and uracil (base of RNA) pairs is interesting because these two molecules have similar monomer properties for electron at-

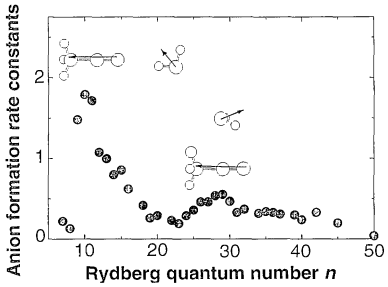

Fig. 2. Dependence on the principal quantum number (n) of the relative rate constants (in arbitrary units) for the formation of water-acetonitrile dimer anions in collisions of Xe (n, $\ell = 3$) Rydberg atoms (where ℓ is the orbital quantum number) with water-acetonitrile clusters, obtained by flowing helium (2 bar) above a mixture of liquid acetonitrile and water. The two peaks correspond to the formation of two different isomer geometrical configurations; arrows indicate the relative dipole moments of the complexes. The corresponding neutral dimers are obtained by field detachment of the anions (40 kV cm^{-1} and 500 V cm^{-1}, respectively, for the large and small dipole configurations).

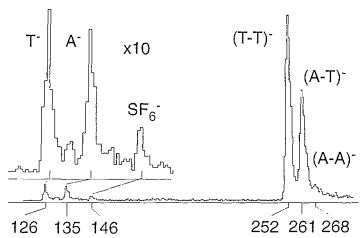

Fig. 3. Mass spectrum of adenine, thymine monomers, dimers, and pair anions. The anions were produced by charge-exchange collisions between a beam of laser-excited Xe (n = 15, ℓ = 3) Rydberg atoms and a helium-seeded beam of A and T molecules. We obtained the molecular beam by heating a 1:1 mixture of A and T at 190°C in a stainless steel oven expanded with helium (700 mbar) through a 50-μm-diameter nozzle, followed by a heated skimmer (100°C) at 20 mm. The collision region is the pulsed acceleration zone of a Wiley-McLaren time-of-flight system. The absolute mass calibration was performed by addition of a small amount of SF_6; the accuracy of anion masses (shown along the bottom) is 0.2 atomic mass units.

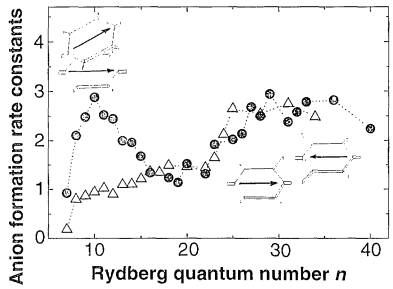

Fig. 4. Dependence on the principal quantum number (n) of the relative rate constants (in arbitrary units) for the formation of anions in collisions between Xe (n, ℓ = 3) Rydberg atoms and T-T (solid circles) or U-U (open triangles) molecular pairs. The peaked feature for thymine around n = 10 is attributed to the production of dipole-bound anions by electron attachment to stacked pairs. At large values of n ($n > 20$), both anion formation rates are identical and are attributed to the formation of H-bonded conventional anions with nearly null resultant dipole moments. Arrows indicate the relative dipole moments of the complexes.

tachment. The presence of a methyl group in thymine, instead of a hydrogen atom in uracil, appears to be an important factor for the isolated pair structure.

We have demonstrated the feasibility of nondestructive selection of mass and geometrical configuration of both neutral and negatively charged polar complexes. In biology, it is often difficult to distinguish between intrinsic properties and environmental effects. The production of supersonic beams of several unmethylated DNA or RNA bases as well as of some of their pairs allowed the experimental determination of the geometries of these pairs and direct comparison to quantum chemical calculations.

REFERENCES

1. U. Buck and I. Ettische, *J. Chem. Phys.* **100**, 6974 (1994).
2. W. Schöllkopf and J. P. Toennies, *Science* **266**, 1345 (1994).
3. K. I. Peterson and W. Klemperer, *J. Chem. Phys.* **81**, 3842 (1984).
4. C. A. Hayman, D. V. Brumbauch, D. H. Levy, *ibid.* **79**, 1581 (1983).
5. O. H. Crawford and W. R. Garret, *ibid.* **66**, 4968 (1977).
6. C. Desfrançois, A. Abdoul-Carime, N. Khelifa, J. P. Schermann, *Phys. Rev. Lett.* **73**, 2436 (1994).
7. J. Simons and K. D. Jordan, *Chem. Rev.* **87**, 535 (1987).
8. H. Haberland, H. Ludewigt, C. Schindler, D. R. Worsnop, *Phys. Rev. A* **36**, 967 (1987).
9. C. Desfrançois, *ibid.* **51**, 3667 (1995).
10. K. Harth, M.-W. Ruf, H. Hotop, *Z. Phys. D* **14**, 149 (1989).
11. C. Desfrançois *et al.*, *J. Chem. Phys.* **102**, 4952 (1995).
12. M. Anbar and G. A. St. John, *Science* **190**, 781 (1975).
13. R. D. Brown, P. D. Godfrey, D. McNaughton, A. P. Pierlot, *J. Am. Chem. Soc.* **110**, 2329 (1988).
14. Y. Tsuchya, T. Tamura, M. Fuji, M. Ito, *J. Phys. Chem.* **92**, 1760 (1988).
15. L. F. Sukhodub, *Chem. Rev.* **87**, 589 (1987).
16. K. Szczepaniak, M. Szczesniak, W. B. Person, *Chem. Phys. Lett.* **153**, 39 (1988).
17. M. Graindourze, J. Smets, T. Zeegers-Huyskens, G. Maes, *J. Mol. Struct.* **318**, 55 (1994).
18. M. D. Sevilla, B. Besler, A. O. Colson, *J. Phys. Chem.* **98**, 2215 (1994).
19. N. A. Oyler and L. Adamowicz, *Chem. Phys. Lett.* **219**, 223 (1994).
20. J. Langlet, P. Claverie, F. Caron, J. C. Boeuve, *Int. J. Quant. Chem.* **19**, 299 (1981).
21. R. Stewart and L. Jensen, *Acta Crystallogr.* **23**, 1102 (1967).
22. M. Aida and C. Nagata, *Int. J. Quant. Chem.* **29**, 1253 (1986).
23. P. Hobza and C. Sandorfy, *J. Am. Chem. Soc.* **109**, 1302 (1987).

4 April 1995; accepted 13 July 1995

Mating Patterns in Malaria Parasite Populations of Papua New Guinea

R. E. L. Paul, M. J. Packer, M. Walmsley, M. Lagog, L. C. Ranford-Cartwright, R. Paru, K. P. Day*

Description of the genetic structure of malaria parasite populations is central to an understanding of the spread of multiple-locus drug and vaccine resistance. The *Plasmodium falciparum* mating patterns from Madang, Papua New Guinea, where intense transmission of malaria occurs, are described here. A high degree of inbreeding occurs in the absence of detectable linkage disequilibrium. This contrasts with other studies, indicating that the genetic structure of malaria parasite populations is neither clonal nor panmictic but will vary according to the transmission characteristics of the region.

Sexual recombination, which is an obligate part of the malaria life cycle in the mosquito vector, is believed to play a significant role in the generation of parasite diversity (*1*) observed in natural parasite populations (*2–4*). Although clonal population structures have been proposed for other parasitic protozoa (*5*) and bacteria (*6, 7*), there are conflicting population genetic data for malaria (*8*). Linkage disequilibrium analyses have been unable to resolve the extent to which the genetic structure of malaria parasite populations deviates from panmixia (*3, 8, 9*). The interpretation of such analyses is easily confounded by the choice of sampling scale (*2, 7, 10*), which in the case of malaria must be defined in relation to the spatial heterogeneity of parasite transmission within a given endemic area (*2*).

Measurement of heterozygosity enables detection of any deviation from Hardy-Weinberg equilibrium, which is expected under random mating conditions. *Plasmodium falciparum* is haploid for most of its life cycle except for a brief period in the mosquito vector. Heterozygosity can easily be detected in the oocyst with gene amplification techniques (*11*). This life cycle stage resides in the mosquito midgut wall and contains the haploid products of meiosis. Laboratory experiments have shown no mating incompatibility between different parasite genotypes (*12*), so detection of oocyst heterozygosity should depend on the number of simultaneously infectious genotypes per human host and the feeding behavior of the anopheline vector. Interrupted feeding and consequent sampling of multiple hosts by the mosquito vector may also contribute to the diversity of parasite genotypes in the blood meal (*13*), although this contribution is considered negligible (*2, 14*).

We have measured oocyst heterozygosity and patterns of genetic linkage disequilibrium in parasite populations of rural Madang, on the north coast of Papua New Guinea (PNG), where intense, all-year-round transmission of malaria occurs. Parasite samples were collected from both human residents and blood-fed mosquitoes in three inland (Umun, Bau, and Sah) and three coastal (Agan, Dogia, and Maraga) villages (*15*) where a fivefold difference in transmission has previously been reported (*16, 17*). Parasite DNA was extracted and amplified for three polymorphic loci: *merozoite surface proteins 1* and *2* (*MSP-1*, *MSP-2*) and the *glutamate-rich protein* (*GLURP*), located on chromosomes 9, 2, and 10, respectively, of the 14 chromosomes of the haploid genome (*18*). These loci were amplified by polymerase chain reaction (PCR) techniques, sized, and probed with allele-specific probes (*11, 19–21*).

Considerable allelic diversity was observed in parasite populations from both human blood and mosquitoes (Fig. 1). There were 14 alleles identified for *MSP-2*, 9 alleles for *MSP-1*, and 9 alleles for *GLURP* in human blood samples. There were 13 *MSP-2* alleles, 8 *MSP-1* alleles, and 7 *GLURP* alleles in the oocysts. A comparison of allele frequencies of the human and oocyst parasite populations within a region (coastal or inland) was carried out independently for each locus: The human parasite populations were significantly different from the oocyst parasite populations for *MSP-2* and *GLURP* ($P < 0.01$) (*22*). Mosquito and human parasite populations share most of the alleles, but they are found at very different frequencies. This suggests that not all infections in the human population were simultaneously and equally infectious. The substantial difference in prevalence of infection in the human (20 to 29% inland, 38 to 51% coastal) compared with the blood-fed mosquito population [1% (*20, 23*)] presumably results from this variable infectiousness of the parasite and the source of the bloodmeal [that is, animal compared with human (*24*)].

Heterozygosity after blood-feeding re-

R. E. L. Paul and K. P. Day, Wellcome Centre for the Epidemiology of Infectious Disease, Department of Zoology, University of Oxford, South Parks Road, Oxford, OX1 3PS, UK.
M. J. Packer, M. Lagog, R. Paru, Papua New Guinea Institute of Medical Research, Post Office Box 378, Madang, Papua New Guinea.
M. Walmsley, Department of Biology, Imperial College, London, SW7 2BB, UK.
L. C. Ranford-Cartwright, Institute of Cell, Animal, and Population Biology, Division of Biological Sciences, University of Edinburgh, Edinburgh EH9 3JT, UK.
* To whom correspondence should be addressed.